Journal of Solid State Chemistry **154,** 177–187 (2000)
doi:10.1006/jssc.2000.8832, available online at http://www.idealibrary.com on IDEAL®

Quantitative Electron Probe Microanalysis of Boron

G. F. Bastin[1] and H. J. M. Heijligers

Laboratory of Solid State and Materials Chemistry, University of Technology, P.O. Box 513, NL-5600 MB Eindhoven, The Netherlands

Received September 9, 1999; in revised form February 4, 2000; accepted February 15, 2000

Quantitative electron probe microanalysis of boron has been performed in 28 binary borides in the range of 4–30 kV. In principle, intensity measurements of ultra-light element radiations can only be performed correctly if the effects of peak shifts and peak shape alterations between specimens and standard are taken into account. The analysis of boron is further complicated by the fact that the peak shape may also be dependent on the crystallographic orientation of the specimen with respect to the electron beam and spectrometer. This was found to be the case in 50% of the compounds investigated. However, if the measurements are performed properly, and if a good matrix correction program is used in conjunction with a consistent set of mass absorption coefficients, it is possible to obtain a narrow error distribution. The final histogram, displaying the number of analyses versus the ratio between calculated and measured intensity ratios that we obtained for 192 analyses with our PROZA96 program, had a root-mean-square value of 3.31% and a mean value of 1.0022. © 2000 Academic Press

Key Words: **EPMA; quantitative microanalysis of boron; ultra-light elements.**

SUMMARY

Quantitative electron probe microanalysis of boron has been performed in 28 binary borides in the range of 4–30 kV. The procedures for accurate intensity measurements of the BK_α line are discussed in detail. It is shown that, similar to the analysis of carbon, it is necessary to perform the intensity measurements in an integral fashion, because of peak shifts and peak shape alterations in the emitted X-ray peak. In the analysis of boron, however, there is an additional problem: peak positions and peak shapes may be dependent also on the crystallographic orientation of the specimen with respect to the electron beam and the position of the spectrometer used. Approximately 50% of the borides were found to exhibit such an effect. This implies that the approach proposed earlier, i.e., the use of a fixed area/peak factor (APF) to deal with peak shape alterations, can be applied only in 50% of the cases in a straightforward manner. In the remaining cases, where the crystallographic orientation of the specimen also plays a role, the variation of APF with peak position (or wavelength) has to be established experimentally.

The present work has resulted in 192 k-ratios for BK_α relative to elemental boron. These data have been used to test our "PROZA96" $\varphi(\rho z)$ matrix correction program, which is based on a double Gaussian $\varphi(\rho z)$ procedure. At the same occasion the available sets of mass absorption coefficients for boron were tested for consistency and better values suggested where necessary. Our correction program was highly successful in the analysis of boron: a relative root-mean-square value of 3.31% was obtained, in combination with a mean k'/k value of 1.0022. Such results can only be achieved, of course, if due care is exercised in the measurements and if the correct analytical procedures are followed.

INTRODUCTION

The rapid developments in the field of materials science call for the simultaneous development or extension of analytical techniques which are capable of performing chemical analyses in microvolumes. Electron probe X-ray microanalysis (EPMA), in which the elements, locally present in such a microvolume, are excited by a finely focused electron beam, after which the emitted X-ray signals are used for qualitative and quantitative analysis, is eminently suited for this purpose. The combination of image-forming capabilities and microanalytical techniques gives the method its distinct and rather unique features, which also explains why the technique is so widely used in materials science laboratories all over the world.

Unfortunately, the new and exotic materials, such as wear-resistant coatings, new ceramic materials, and superconductors, which are developed and introduced at an ever increasing rate, often contain ultra-light elements, like boron, carbon, nitrogen, and oxygen and quantitative EPMA of these elements is not a straightforward matter.

[1]To whom correspondence should be addressed. E-mail: G.F. Bastin@tue.nl. Fax: (+ 31) 40-2445619.

0022-4596/00 $35.00

It is the purpose of the present paper to discuss the specific problems in the analysis of ultra-light elements, and that of boron in particular, and to compare the analytical procedures to those used in the analysis of medium-to-high atomic number elements.

ANALYTICAL PROCEDURES

The routine procedure, which is followed in day-to-day practice in EPMA of medium-to-high atomic number elements, consists of three basic steps:

(a) Specimen preparation.
(b) Intensity measurement, in which the intensity of a selected X-ray line emitted by the specimen is compared to that of a suitable standard. The ratio between the intensities (k-ratio) is finally used in the last step as input for the quantification procedure.
(c) Matrix correction, in which the measured k-ratios are converted into suitable concentration units.

For matrix correction a number of good correction programs have emerged (1–9) in the past two decades or so. Especially the so-called $\varphi(\rho z)$ programs, which are based upon the use of realistic descriptions of the number of X-ray photons (φ) produced as a function of mass depth (ρz) in the specimen, have proved to be extremely powerful.

However, as we have pointed out on a number of occasions (10–14), matrix correction is not a matter of the correction program alone. The reliability of the mass absorption coefficients (mac's), the magnitude of which plays a crucial role in the absorption correction scheme, is of equal importance. In this context it has to be realized that it is difficult enough to find agreement within 10% between experimentally determined mac values quoted by various sources in literature (15–20) for wavelengths as short as those of AlK_α or SiK_α (approx. 7–8 Å) in an absorber such as Ni. Knowing this, it is not difficult to imagine how large the uncertainty will be for the wavelength of 67.6 Å of the BK_α line. This is illustrated in Table 1, where the values from three independent sources are compared to the values we propose, and which are based on the EPMA measurements presented in this paper. Taking into account that a 1% variation in the mac for BK_α in a given absorber produces a 1% variation in the final result, it will be obvious that in EPMA one cannot take any arbitrary set of mac's for granted.

TABLE 1
Mass Absorption Coefficients for Boron-K_α X Rays According to Various Sources

Absorber	Henke (18)	Henke (19)	Henke (20)	Present work
B	3353	3350	3350	3350
C	6456	6350	6400	6450
N	10570	11200	10900	10400
O	16530	16500	18500	16500
Al	65170	64000	77300	64000
Si	74180	84000	86100	81400
Ti	15280	15300	16800	15100
V	16710	16700	19900	18250
Cr	20670	20700	22400	20200
Fe	25780	27600	31000	27000 (?)
Co	28340	30900	30900	33000 (?)
Ni	33090	35700	39600	41500 (?)
Zr	38410[a]	8270	7240	4330
Nb	4417	6560	5470	4600
Mo	4717	5610	5710	4400
La	3826	3730	3400	2900
Ta	20820	20800	20800	21800 (?)
W	19660	19700	19400	20400 (?)
U	2247	9020	9600	8000 (?)

[a]Value obviously extrapolated over M-5 absorption edge.

Special Requirements for Ultra-light Elements

Step 1: *Specimen preparation.* This very first step in the analytical procedure is of vital importance for the analysis of ultra-light elements, because X-ray generation and certainly X-ray emission take place in extremely shallow volumes under the specimen surface. This is illustrated in Fig. 1, where the $\varphi(\rho z)$ curve for BK_α radiation in AlB_2 is shown at an accelerating voltage of 10 kV. Due to the huge absorption of BK_α X-rays (mac's BK_α/B, 3350; BK_α/Al, 64,000 cm^2/g) there is a tremendous difference between the curves for the generated and emitted intensities. With a density of 3.19 g/cm^3 it is easy to calculate that half of the emitted intensity comes from a linear depth of less than 1000 Å, or 0.1 μm. It is not difficult to see then that the preparation of the specimen surface is of the utmost importance: any interference of superficial contaminants or oxide skins with the X-ray emission volume is disastrous for the analysis. Likewise, it will be obvious that the flatness of the specimen is of extreme importance in view of the correctness of the X-ray take-off angle.

Step 2: *Intensity measurement.* The routine procedure in wavelength-dispersive EPMA is that the net peak intensities obtained from specimen and standard are compared and the ratio between these emitted intensities (k-ratio) is used as the input parameter for the matrix correction program. This procedure is, in fact, based upon the tacit assumption that the peak intensity is a good measure for the integral emitted intensity of the X-ray photons, associated with a specific electronic transition within the atom. This can only be true, of course, if the shapes of the peaks emitted by the specimen and the standard are exactly the same. While this is the case for the vast majority of X ray lines from medium-to-high atomic number elements ($Z > 11$), it

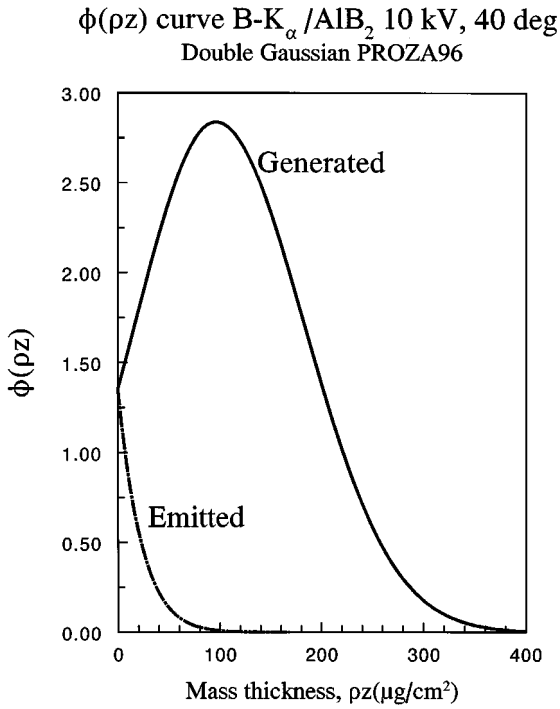

FIG. 1. $\varphi(\rho z)$ curve for BK_α radiation in a highly absorbing system, e.g., in AlB_2. The solid curve represents the generated intensity; the broken curve the emitted intensity. Note that the emitted intensity is almost exclusively due to the surface ionization $\varphi(o)$ and the very first part of the $\varphi(\rho z)$ curve. Accelerating voltage, 10 kV; X-ray take-off angle, 40 deg. Mass absorption coefficients for BK_α: in Al, 64,000; in B, 3350 cm^2 g.

is no longer true for ultra-light elements and, perhaps, not for soft X-rays in general. The excitation of X rays in ultra-light elements is the result of transitions by electrons, which are involved in the chemical bond. As a result, we must expect the following.

(1) *Peak shifts*: These effects are easily accounted for by a careful peak search every time the electron beam is moved from specimen to standard. However, the operator needs to be aware of these effects.

(2) *Peak shape alterations*: This is the real problem in quantitative EPMA of ultra-light elements, because it is *not* easily accounted for. In principle, it becomes necessary to perform all intensity measurements in an integral fashion, which is not an attractive option with a WDS spectrometer.

We have demonstrated the large differences that can occur between emitted peak shapes previously in the case of carbon (10–12). When, for example, the CK_α peaks emitted by TiC and vitreous carbon are scaled to the same net peak height it becomes obvious that an intensity measurement purely at the maximum of the peak must lead to the wrong answer. Since the peak from vitreous carbon is twice as broad as that from TiC, it is clear that the intensity emitted from TiC is overrated by a factor of 2. In such a case the only correct procedure is an integral intensity measurement, which would lead to the correct integral (area) k-ratio (AKR), rather than the wrong peak k-ratio (PKR).

In our previous work we have also shown that there is a fixed ratio between area and peak k-ratio for the peak emitted from a specific compound, relative to a specific standard, and we have called this ratio the area/peak factor (APF). Once an APF is known for a particular compound, further measurements can be done very rapidly on the peak again and simple multiplication of the PKR with the APF will yield the correct integral (area) k-ratio AKR.

The experimental evidence we collected in the case of carbon shows that the APF values are virtually independent of accelerating voltage; therefore, these values can be determined at the best possible voltage and can further be used throughout the full voltage range of interest. A most conspicuous feature was the pronounced sawtooth-like variation of APF we observed with the atomic number of the metal partner in the carbides we investigated. Strong carbide-formers, such as TiC and ZrC, showed the lowest APF values (relative to Fe_3C as a standard), which means extremely narrow peaks, with relatively high peak intensities.

For conceptual purposes the APF can be regarded as some kind of width-to-height ratio in a peak. However, under no circumstances should it be confused with the full-width-at-half-maximum (FWHM) of a peak, because most peak broadening (shape alteration) effects take place at the foot of the peak and such effects would go unnoticed in a FWHM measurement. Probably the best way to look at the APF is to consider it as a weight, which has to be assigned to a specific emission peak, if this is measured at the maximum of the peak.

It must be emphasized that the APF is dependent on the analyzer crystal and the resolution of the spectrometer (diameter of the Rowland circle). Two final remarks:

(1) The APF is defined relative to a specific standard.

(2) The APF is not a universal physical constant which can be transferred blindly to another instrument.

Additional Problems in the Analysis of Boron

Turning to the analysis of boron, a number of the experimental and fundamental problems, described previously for carbon, had to be anticipated for boron, too. However, the research we carried out on 28 binary borides showed some additional problems. Apparently, there are two types of borides:

(1) Type A. The borides of this type behave exactly the same as the carbides we investigated; they exhibit a fixed peak shift and a fixed peak shape alteration relative to the elemental boron standard used. Examples in this group are BN (hexagonal and cubic), LaB_6, and UB_4. Approximately 50% of the borides we investigated belong to this group.

(2) Type B. The borides in this group exhibited a most peculiar effect in that the peak position and the peak shape were observed to be dependent on the crystallographic orientation of the specimen with respect to the electron beam and the spectrometer used. When the specimen was rotated in its own plane under the electron beam the emitted BK_α peak was found to shift back and forth and the shape of the peak was varying all the time. The narrowest peak, with the highest peak intensity, was always found at the shortest wavelength and vice versa.

The most pronounced examples of these crystallographic effects were found in compounds such as TiB and ZrB_2 (Fig. 2). The figure clearly shows the two extremes that we observed in the peak shapes emitted from ZrB_2. The peak shift in this case is about 1 mm, corresponding to 0.35 Å. The measured peak *k*-ratio, relative to elemental boron, shows a strong decrease (Fig. 3, top) with the observed peak position on the stearate analyzer crystal. The integral (area) *k*-ratio, on the other hand, shows a tendency to take a more or less constant value (within experimental error). As a result, the APF value for ZrB_2 (Fig. 3, bottom) shows a strong, almost parabolic variation with peak position. This example shows, by the way, that it is extremely dangerous even to take the same ZrB_2 specimen as an (internal) standard, even if a careful peak search is performed between measurements on different crystallographic grains in the specimen. The operator simply has to be aware of the crystallographic effects, and the associated alterations in the peak shapes, and he has to assign the proper "weight" (APF) to the peak intensity, measured at a specific position of the analyzer crystal. Table 2 gives a complete survey of the

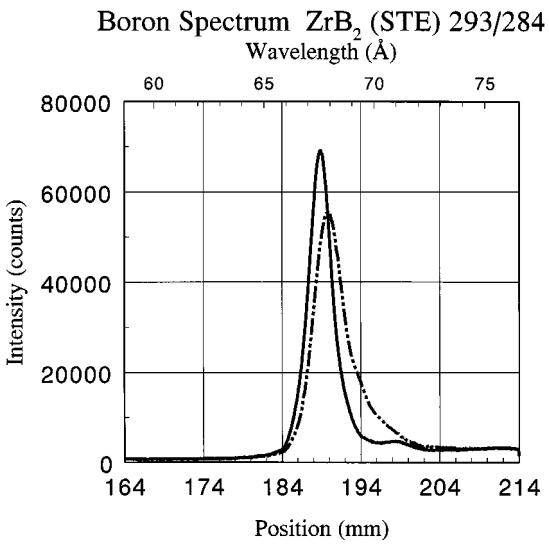

FIG. 2. Two extremes that can be observed in the shape of the BK_α peak emitted by ZrB_2 upon rotating the specimen in its own plane under the electron beam.

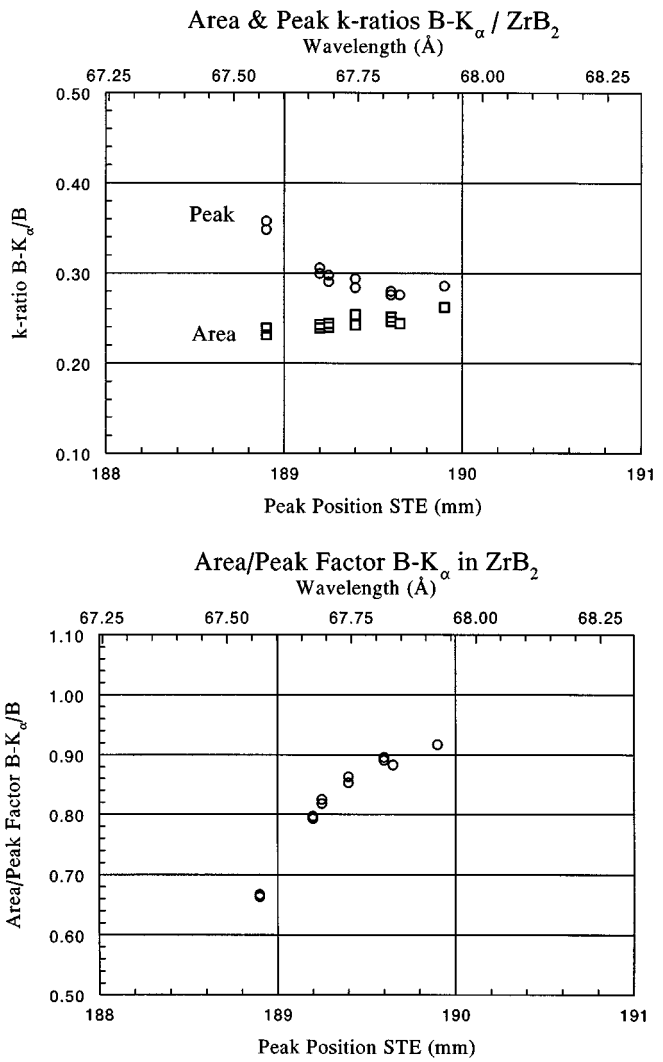

FIG. 3. Variation of area (integral) and peak *k*-ratio for BK_α (top) and area/peak factor (bottom) with detected peak position on lead stearate in ZrB_2 (hexagonal) as a typical representative of the noncubic borides.

APFs, measured on a conventional lead stearate crystal in the present investigation. Single values are characteristic for type A borides, while the ranges, reported for type B borides, correspond to the maximum variation in APF we observed with detected peak position. The global variation of APF with atomic number of the alloying element shows the same strong sawtooth-like behavior as we reported earlier for the analysis of carbon (10–12). Combinations of boron with elements such as titanium or zirconium again lead to the emission of narrow peaks, with relatively high peak intensities. This trend is clearly visible in Table 2, despite the large variation in APF that these compounds can exhibit.

The origin of these most peculiar peak shape alterations in dependence of the crystallographic orientation of the

TABLE 2
Area/Peak Factors for BK_α Radiation Relative to Boron for the Lead-Stearate Crystal

Boride	APF	Peak. pos. (mm)	Wavelength (Å)
B	1.000 (def.)	189.00	67.60
B_4C	1.014 (27)	189.00	67.60
BN (Hex)	1.198 (9)	191.05–191.60	68.33–68.53
BN (Cub)	1.192 (14)	190.10	67.99
B_6O	1.145 (8)	188.74	67.51
AlB_2	1.152–1.095 (7)	189.50–189.90	67.78–67.92
AlB_{12}	1.008 (9)	189.03	67.61
SiB_3	1.003 (5)	188.85	67.55
SiB_6	0.922 (5)	189.00	67.60
TiB	0.690–0.835 (12)	188.80–189.45	67.53–67.76
TiB_2	0.799–0.945 (12)	189.35–190.25	67.73–68.05
VB_2	0.950–1.045 (9)	189.85–190.70	67.91–68.21
CrB	0.825–1.000 (19)	189.25–190.25	67.69–68.05
CrB_2	0.950–1.090 (10)	189.90–190.90	67.92–68.28
Fe_2B	1.242 (6)	188.90	67.57
FeB	0.985–1.160 (11)	189.55–190.00	67.80–67.96
Co_2B	1.015 (5)	189.10	67.64
CoB	1.186 (5)	190.40	68.10
Ni_3B	1.020–0.935 (7)	189.40–189.85	67.74–67.91
Ni_2B	1.059 (14)	189.10	67.64
NiB	1.060–1.310 (18)	189.80–190.45	67.89–68.12
ZrB_2	0.665–0.915 (13)	188.90–189.90	67.57–67.92
NbB	0.775–0.855 (7)	189.05–189.55	67.62–67.80
NbB_2	0.810–1.025 (9)	189.50–190.55	67.78–68.16
MoB	0.936 (4)	189.70	67.85
LaB_6	0.898 (6)	189.55	67.80
TaB	0.853–0.881 (5)	189.55–189.85	67.80–67.91
TaB_2	0.990–1.120 (8)	189.95–190.60	67.94–68.17
WB	0.978 (5)	189.80	67.89
UB_4	1.028 (6)	189.95	67.94

Note. The figures in parentheses are the number of measurements on which the data are based.

specimen must be sought in *polarization effects* (21), which may be present in the emitted BK_α radiation. Polarization takes place in two mutually perpendicular directions, which are aligned along the principal crystallographic directions in the specimen crystal. Unfortunately, the analyzer crystal in the WDS spectrometer can act as a polarization filter and by varying the orientation of the specimen with respect to the analyzer crystal parts of the BK_α radiation can be filtered out. It is even more unfortunate that the optimum filtering action is achieved for an angle of incidence of the X rays on the crystal of 45°. This angle is very closely approached in the microprobe we used in the present investigation: a JEOL 733 Superprobe, originally equipped with a conventional lead stearate crystal (STE, 2*d*-spacing of approx. 100 Å). With a wavelength of 67.6 Å for BK_α an angle of incidence of 42.5° is calculated.

In principle, the polarization effects, described here, are possible in all noncubic borides and it must be expected that they are worst when the 2*d*-spacing of the analyzer crystal approaches a value of 95.6 Å. The impact on the actual analysis of boron, in terms of shape alterations and their consequences for the intensity measurements, will be worst when the spectral resolution of the crystal is at its best. It is, therefore, worthwhile to look for another analyzer crystal with a much larger 2*d*-spacing, which would move the BK_α peak away from its present dangerous position on stearate. Strange as it may seem at first sight, it would also be worthwhile to search for a crystal with a poorer spectral resolution than stearate, which would make it less sensitive

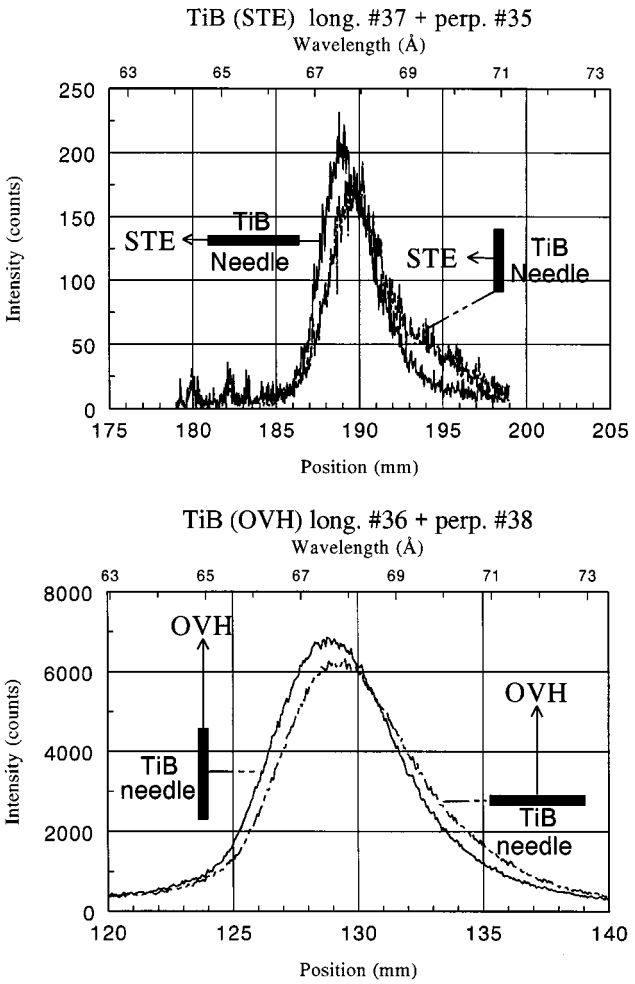

FIG. 4. Peak shape alterations in dependence on the crystallographic orientation of a needle-shaped TiB crystal, simultaneously recorded on STE (top) and OVH (bottom). In both cases the spectra have been recorded once with the TiB needle pointing in the direction of the spectrometer and once in a direction perpendicular to it. The highest peak intensity (at the shortest wavelength) is always found when the needle points in the direction of the spectrometer. Accelerating voltage, 10 kV; beam current, 100 nA; counting time, 1 sec/channel. Note the huge difference in count rate between the STE and OVH crystals.

TABLE 3

Area/Peak Factors for BK_α Radiation Relative to Elemental Boron: Comparison between Lead-Stearate (STE) and OVH (Mo/B_4C) Crystal

Boride	STE	OVH
B_4C	1.014	1.061
AlB_2	1.152–1.095	1.054
TiB	0.690–0.835	0.855–0.915
TiB_2	0.799–0.945	0.922–0.965
Fe_2B	1.242	1.085
ZrB_2	0.665–0.915	0.904–0.948
LaB_6	0.898	0.951

to shape alterations. Both requirements can be met currently by the selection of one of the modern synthetic multilayer crystals (22), which can be purchased commercially in a large range of 2*d*-spacings, and which are often optimized for a (small) range of (ultra-light) elements. For the analysis of BK_α (and BeK_α) a Mo/B_4C crystal (code name OVH) with a 2*d*-spacing of 145 Å was acquired, and for some time we had this crystal and the conventional stearate (STE) crystal in two separate vertical spectrometers, mounted at an angle of approx. 90° between them.

This particular configuration enabled us to do some rather unique experiments on a TiB sample, consisting of fine TiB needles, grown in a Ti-rich matrix. In the first part of the experiment the axis of one of the needles, representing, of course, an important crystallographic direction, was directed toward the spectrometer containing the STE crystal and BK_α spectra were recorded on STE and OVH crystals (Fig. 4). Then, the needle was rotated over 90° and the experiment was repeated. It is obvious that in both situations the narrowest peak with the highest peak intensity is achieved when the direction of take-off of the X rays is in the plane formed by the electron beam and the needle axis. A maximum shift to the left on one crystal means automatically a maximum shift to the right for the other, with a corresponding variation in peak shape. Figure 4 also shows, by the way, that the resolution of the OVH crystal is definitely worse than that of the STE crystal, because the

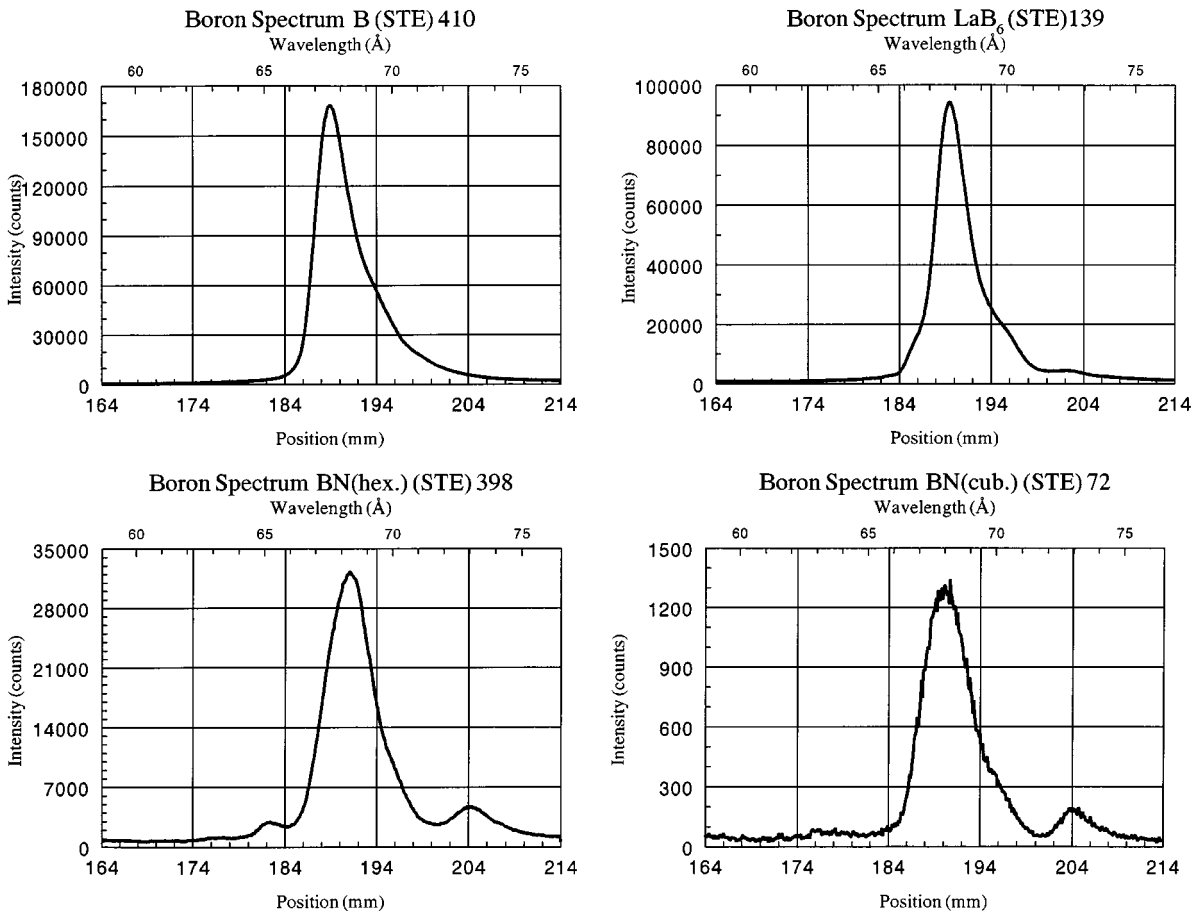

FIG. 5. BK_α spectra recorded with the stearate crystal (STE) from B, LaB_6, and hexagonal and cubic BN. Note the fine detail that can be resolved and the peculiar differences between the peak shapes emitted by the two BN compounds.

peak is much broader. The measurements of APF values on OVH for a selected group of borides (Table 3) emphasize these differences in resolution. Almost without exception, the APF values on OVH are much closer to unity, thus showing that the alterations in the peak shape on OVH are much smaller than on STE. The fine details that can be resolved with a STE crystal are exemplified in Fig. 5 for three borides, compared to elemental boron. In a number of cases the presence of three components is discernible in the peak. The most conspicuous feature in Fig. 5 is the remarkable difference in the appearance of the BK_α peak between cubic and hexagonal BN: in the former compound one of the "side wings" is missing. However, it should be noticed that *all* components in both spectra should be included in an integral measurement. If this is done, the APF values (Table 2) are virtually the same, meaning that the integral emitted intensity is the same.

The loss in spectral resolution with an OVH crystal is demonstrated graphically in Fig. 6, which shows that the three components in the BK_α peak are no longer discernible with OVH. On the other hand, it must be emphasized that the count rates obtained with the OVH crystal can be as much as 30 times those of the STE crystal (see Fig. 4). Therefore, in those cases where there is no danger of spectral interference, it is extremely beneficial to use the OVH crystal, because it couples a much higher count rate with a much lower sensitivity to peak shape alterations. In a few isolated cases, however, notably in combinations of boron with Nb or Mo, the use of OVH could lead to large interpretation errors, because, e.g., the presence of the MoM_ζ line in the immediate vicinity of the BK_α line would be completely overlooked (Fig. 7).

Measurements of Intensities and Peak and Integral k-Ratios for Boron

Full details on specimen preparation and experimental procedures can be found in one of our previous publications (23). Once the APFs were known (type A borides), or the variation of APF with peak position (type B), large numbers of relatively fast peak *k*-ratios could be measured with STE over a wide range in accelerating voltages. In cases of not

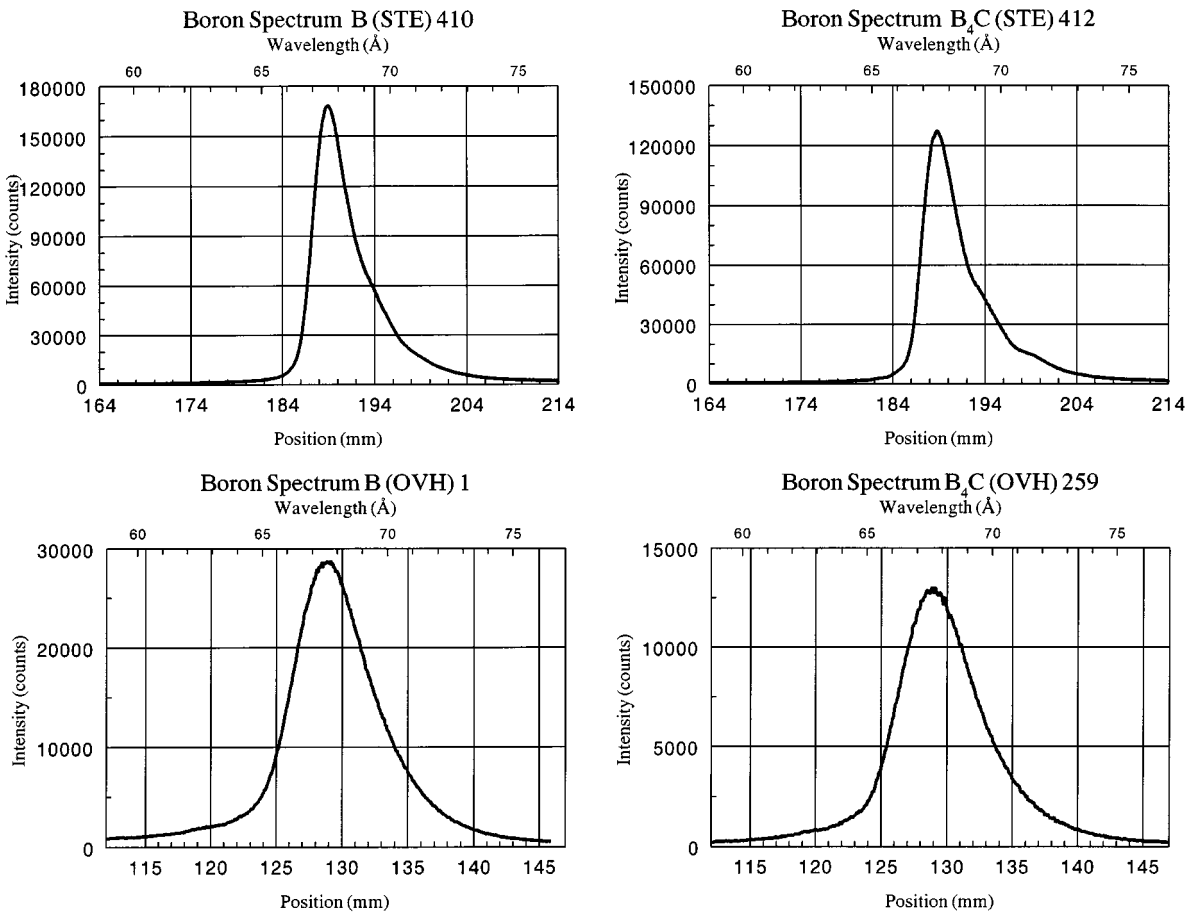

FIG. 6. Differences in spectral resolution between the stearate (STE) crystal (top) and the synthetic Mo/B_4C multilayer crystal (OVH, bottom) for boron (left) and B_4C (right).

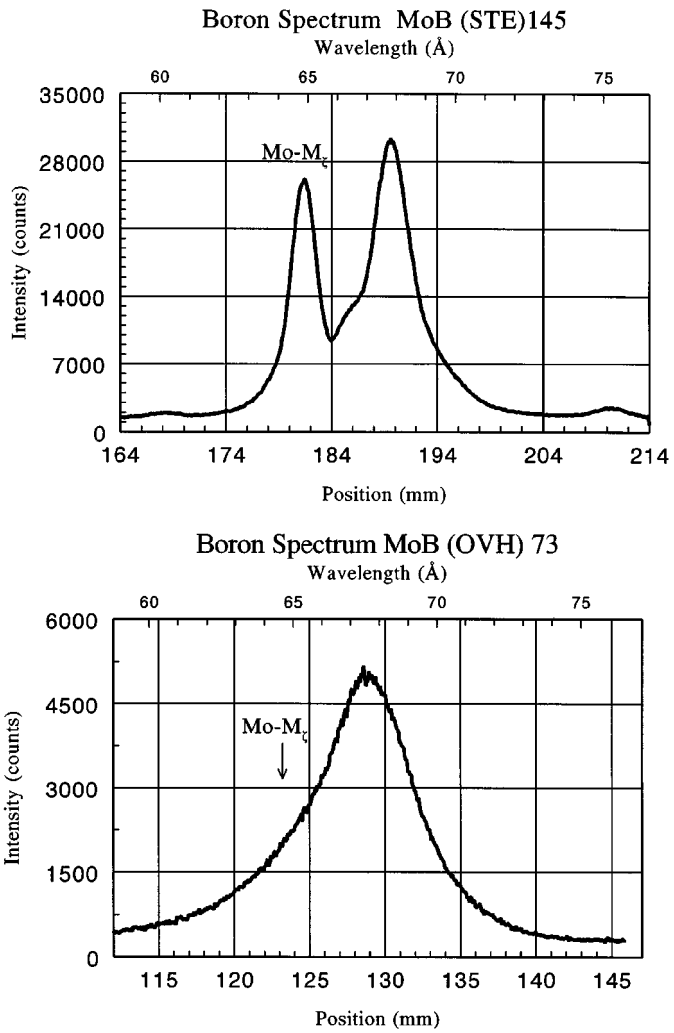

FIG. 7. Severe loss in spectral resolution by the OVH crystal. In contrast to the STE crystal the MoM_ζ peak can no longer be resolved from the BK_α peak by OVH.

too heavy absorption this range started at 4 kV and extended up to 30 kV; in the remaining cases the upper limit was 15 kV. Subsequent multiplication of the peak *k*-ratios with the appropriate APF values finally yielded the correct integral *k*-ratios.

In order to appreciate the reduction in time that can be achieved using this procedure it must be realized that under the conditions (number of steps, counting time, step size) we applied, apart from the standard, only four boride spectra could normally be measured during one night. If the range 4–30 kV has to be measured at nine different voltages, then two weeks would be necessary for each boride specimen and still the statistics would be very poor, with only four integral *k*-ratios for each voltage. Using the APF concept this full range can be measured in much less than a day and with much better statistics.

A number of representative measurements (over the full range in accelerating voltage) are given in Figs. 8 and 9, where the measured integral *k*-ratios for BK_α are compared to the predictions of our correction program "PROZA96" (8), using the mass absorption coefficients quoted. These predictions are the results of matrix correction procedures, which will be the subject of the next sections.

Determination of Consistent Mass Absorption Coefficients for BK_α Radiation

As we have mentioned already, matrix correction in the case of ultra-light elements is just as much a matter of the correction program, as well as of the correctness, or rather

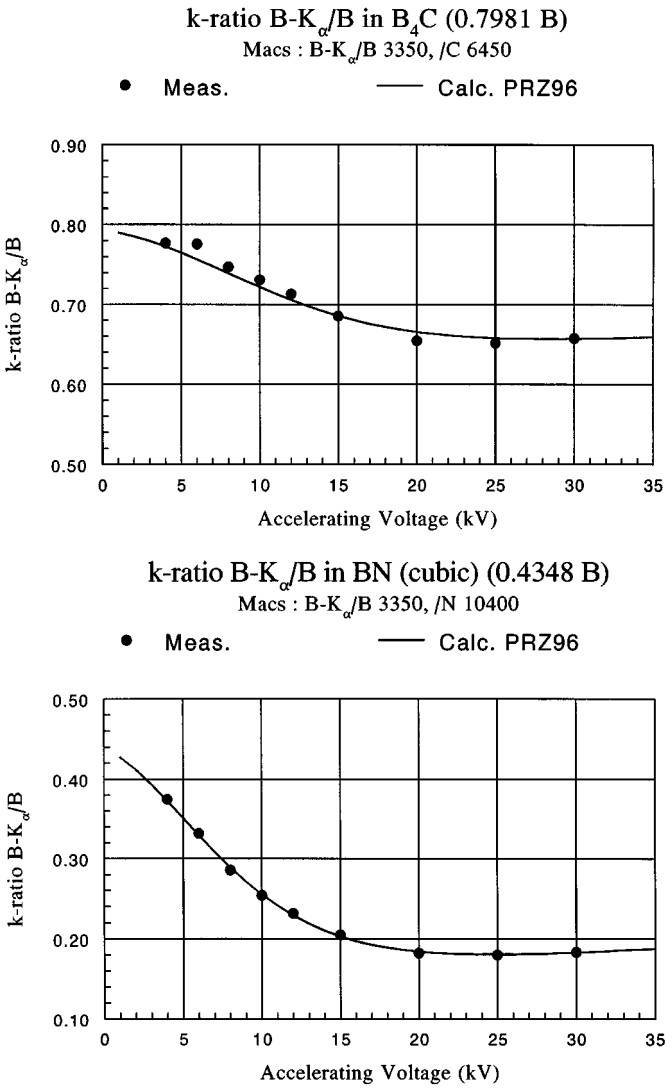

FIG. 8. Intensity ratios for BK_α (integral) as a function of accelerating voltage for B_4C (top) and cubic BN (bottom). Dots represent our measurements and the curves the predictions of our PROZA96 correction program, using the mac's indicated.

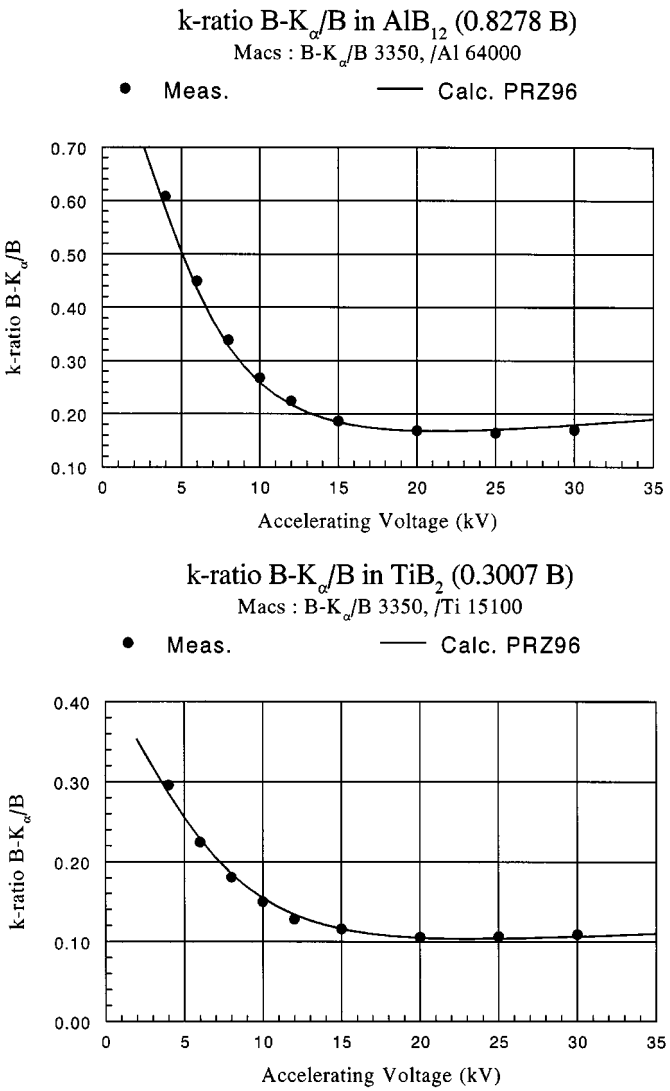

FIG. 9. Intensity ratios for BK_α (integral) as a function of accelerating voltage for AlB_{12} (top) and TiB_2 (bottom). Dots represent our measurements and the curves the predictions of our PROZA96 correction program, using the mac's indicated.

the consistency, of the mass absorption coefficients used. In principle, mac's are required with a relative precision of 1% in order to produce results within 1% precision. While mac values for K_α radiations of elements with atomic numbers higher than 11 range from 100 to several thousands cm^2/g, those of ultra-light radiations may take exceedingly high values indeed. A value for BK_α radiation in Si ranging between 74,000 and 86,000 cm^2/g has been reported in the literature (Table 1). There is little hope that experimental mac values of this nature will ever be available with the required precision: in unfavorable cases values quoted by different literature sources may differ by more than 100%.

Fortunately, we can use EPMA procedures to produce better, or rather, more consistent mac values to work with and, in principle, there are two different ways to achieve this goal. Both methods are based upon the use of a good correction program in combination with an extended set of reliable and reproducible measurements on good specimens over a wide range of accelerating voltages.

In the first method it is necessary to know the composition of the specimen accurately and the measured *k*-ratios are compared with the values calculated by the particular correction program used, in conjunction with a specific set of mac's. The results of such a procedure are, in fact, shown in Figs. 8 and 9. If a too high mac value had been used there would be a growing discrepancy between measurements and calculations, in the sense that with increasing voltage increasingly too low *k*-ratios would be calculated, and vice

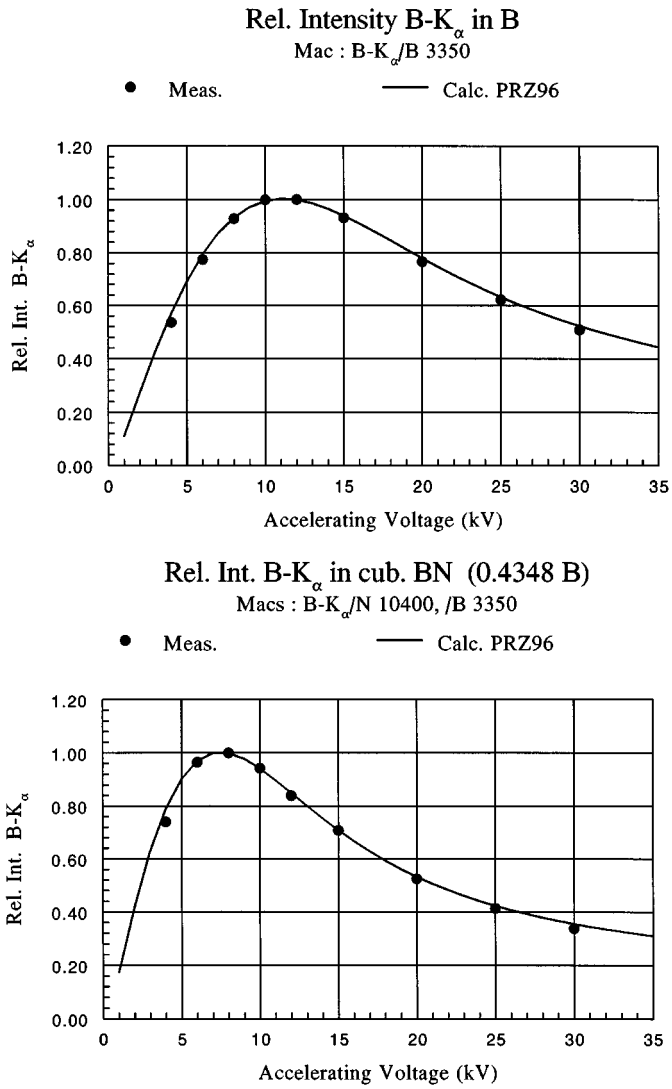

FIG. 10. Relative emitted intensity for BK_α from boron (top) and cubic BN (bottom) as a function of accelerating voltage. Dots represent our measurements and the curves the predictions of our PROZA96 correction program, using the mac's indicated.

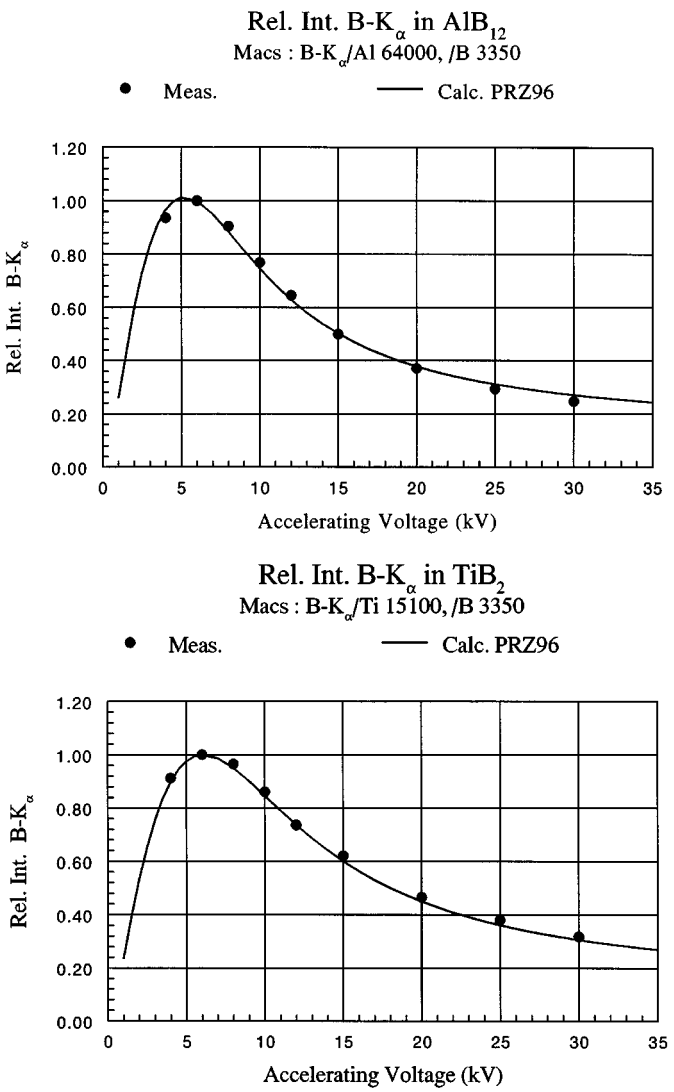

FIG. 11. Relative emitted intensity for BK_α from AlB_{12} (top) and TiB_2 (bottom) as a function of accelerating voltage. Dots represent our measurements and the curves the predictions of our PROZA96 correction program, using the mac's indicated.

versa. A slight disadvantage of this method is that the composition of the specimen has to be known fairly accurately.

The alternative method is to measure the relative intensity of the emitted radiation as a function of accelerating voltage and to compare it with the calculations made with a good $\varphi(\rho z)$ correction program, using a variety of mac values. With increasing voltage the maximum in $\varphi(\rho z)$ (see Fig. 1) increases in height and at the same time it shifts toward larger mass depths. Integration of the curve for the emitted intensity gives, after multiplication with the ionization cross-section for the X-ray line in question at the voltage used, a measure for the emitted intensity. After an initial increase in emitted intensity a maximum will be reached after which a decrease sets in again. After suitable scaling, plots like those shown in Figs. 10 and 11 are typically obtained. The position of the maximum in such plots is very sensitive to the magnitude of the mac value in the compound in question and rather insensitive to the composition of the specimen.

If the results in Figs. 8 and 9 and those in Figs. 10 and 11 are inspected it is clear that a very high level of consistency and reliability is obtained indeed in the present investigation. Both procedures have been used to produce the final set of mac's we propose in Table 1.

FINAL RESULTS

The last step in the complete procedure is the conversion of measured k-ratios into suitable concentration units, for which we used our own "PROZA96" $\varphi(\rho z)$ matrix correction program (8). The calculations were made using the mac values for BK_α, proposed in Table 1. The usual test on the performance of a particular correction program is to apply it to a database, consisting of reliable measurements on well-characterized specimens of known compositions, carried out over a wide range of accelerating voltages. For each entry in the database the k-ratio (k') is calculated for the particular composition and accelerating voltage reported, and compared to the measured one (k). It is then common practice to display the ratio k'/k in a histogram showing the number of analyses versus k'/k. The narrowness in the distribution, in terms of the relative root-mean-square error (%), and the mean k'/k ratio are then used as a final measure of success. Figure 12 shows the results obtained with our correction program on the 192 boron measurements compiled in the present investigation. The results speak for

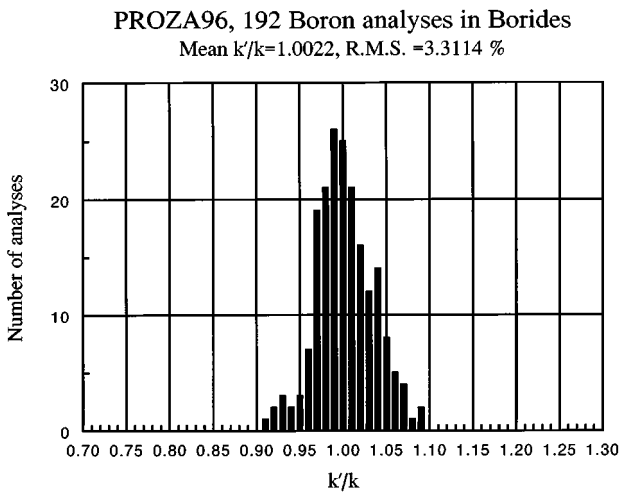

FIG. 12. Performance of our PROZA96 matrix correction program on a database containing 192 boron analyses in binary borides. The number of analyses has been plotted vs the ratio between the calculated and the measured k-ratio for the given composition and accelerating voltage in the database.

themselves: a narrow distribution, well centered on 1, is obtained. It must be emphasized, however, that it is impossible to achieve such results if the program (or any other program for that matter) is forced to operate with one of the published sets of mac values from literature (Table 1). The cases of largest uncertainty are those where the wavelength of BK_α is very close to the M_5 absorption edge, which is the case for absorbers such as Zr, Nb, and Mo.

CONCLUSIONS

The present work shows that quantitative electron probe microanalysis of an ultra-light element such as boron is possible with surprisingly good results. This can only be achieved, however, if

(1) extremely good care is exercised during the measurements, and

(2) a reliable matrix correction program is used, in combination with a set of consistent mass absorption coefficients.

It has to be kept in mind that all steps involved in the complete procedure, beginning with (1) the specimen preparation, then (2) performing correct intensity measurements (peak shapes), and, finally, (3) applying reliable matrix correction procedures (using consistent mac's), are of equal importance.

It will also have to be realized that the actual procedures, involved in quantitative EPMA of ultra-light elements, will always be much more time-consuming than in the analysis of heavier elements.

REFERENCES

1. J. L. Pouchou and F. Pichoir, Parts I and II, *Rech. Aérosp.* **3,** 13 (1984) and **5,** 349 (1984).
2. R. H. Packwood and J. D. Brown, *X-ray Spectrom.* **10,** 138 (1981).
3. G. F. Bastin, H. J. M. Heijligers, and F. J. J. van Loo, *Scanning* **8,** 45–67 (1986).
4. J. L. Pouchou and F. Pichoir, *in* "Proceedings of the 11th International Congress on X-ray Optics and Microanalysis" (J. D. Brown and R. H. Packwood, Eds.), p. 249. Graphic Services, U.W.O, London, Canada, 1986.
5. J. L. Pouchou, F. Pichoir, and D. Boivin, *in* "Proceedings of the 12th International Congress on X-ray Optics and Microanalysis, Cracow, Poland 1989," (S. Jasienska and L. J. Maksymowicz, Eds.,), Cracow, Acad. of Mining and Metallurgy, p. 52 (1990). Also available as ONERA report #TP 1989–157.
6. G. F. Bastin and H. J. M. Heijligers, *in* "Electron Probe Quantitation, Workshop at the Natonal Bureau of Standards, Gaithersburg, Maryland 1988" (K. F. J. Heinrich and D. E. Newbury, Eds.), pp. 145–161, Plenum, New York, 1991.
7. C. Merlet, *Inst. Phys. Conf. Ser.* **130,** Chap. 2, 123–126 (1992).
8. G. F. Bastin, J. M. Dijkstra, and H. J. M. Heijligers, *X-Ray Spectrom.* **27,** 3–10 (1998).
9. V. D. Scott and G. Love, *in* "Electron Probe Quantitation, Workshop at the Natonal Bureau of Standards, Gaithersburg, Maryland, 1988" (K. F. J. Heinrich and D. E. Newbury, Eds.), pp. 19–30. Plenum, New York, 1991.
10. G. F. Bastin and H. J. M. Heijligers, "Quantitative Electron Probe Microanalysis of Carbon in binary Carbides," Internal Report, ISBN 90-6819-002-4. University of Technology, Eindhoven, 1984.
11. G. F. Bastin and H. J. M. Heijligers, *Microbeam Anal.* 291 (1984).
12. G. F. Bastin and H. J. M. Heijligers, *X-Ray Spectrom.* **15,** Parts I and II, 135–150 (1986).
13. G. F. Bastin and H. J. M. Heijligers, *Scanning* **13,** 325–342 (1991).
14. G. F. Bastin and H. J. M. Heijligers, *Mikrochim. Acta*, Suppl. 12, 19–36, (1992).
15. K. F. J. Heinrich, *in* "The Electron Microprobe" T. D. McKinley, *et al.* Eds.), p. 296. Wiley, New York, 1966.
16. K. F. J. Heinrich, *in* "Proceedings of the 11th International Congress on X-ray Optics and Microanalysis" (J. D. Brown and R. H. Packwood, Eds.) p. 67 Graphic Services, U.W.O, London, Canada, 1986.
17. J. Z. Frazer, "A Computer Fit to Mass Absorption Coefficient Data," Publication 67–29. Inst. for the Study of Matter, Univ. of California, La Jolla, 1967.
18. B. L. Henke and E. Ebisu, *Adv. X-ray Anal.* **17,** 150–213 (1974).
19. B. L. Henke, *et al.*, *At. Data Nuclear Data Tables* **27,** 1–144 (1982).
20. B. L. Henke, E. M. Gullikson, and J. C. Davies, *At. Data Nuclear Data Tables* **54,** 181–342 1993.
21. G. Wiech, *in* "X-ray emission spectroscopy" (P. Day, Ed.), Emission and Scattering Techniques Series C, pp. 103–151 NATO Adv. Study Inst., D. Reidel Publishing Co., 1981.
22. G. F. Bastin and H. J. M. Heijligers, *in* "X-Ray Spectrometry in Electron Beam Instruments," (D. Williams, J. Goldstein, and D. Newbury, Eds.) p. 239, Plenum, New York, 1995.
23. G. F. Bastin and H. J. M. Heijligers, "Quantitative Electron Probe Microanalysis of Boron in Binary Borides," Internal Report, ISBN 90-3860-898-5. University of Technology, Eindhoven, 1986, 1997.